RSC Advances

PAPER

View Article Online
View Journal | View Issue



Cite this: *RSC Adv.*, 2016, **6**, 44087

# Synthesis of multi-ion imprinted polymers based on dithizone chelation for simultaneous removal of $Hg^{2+}$, $Cd^{2+}$, $Ni^{2+}$ and $Cu^{2+}$ from aqueous solutions†

Junqing Fu,[ab] Xiaoyan Wang,[bc] Jinhua Li,*[b] Yangjun Ding[a] and Lingxin Chen*[ab]

Simultaneous analysis and removal of various heavy metal ions has received increasing concerns because they are usually co-existent with different toxicological effects. Ion imprinted polymers (IIPs) can effectively identify water-soluble ions especially heavy metal ions, however, multi-ion imprinting is rarely performed owing to possible cross-reactivity and matrix interferences. In this work, a novel and generally applicable IIPs strategy was proposed for simultaneous preconcentration and removal of four heavy metal ions based on dithizone chelation. Multi-ion imprinted polymers (MIIPs) embedded in a sol–gel matrix were prepared by using $Hg^{2+}$, $Cd^{2+}$, $Ni^{2+}$ and $Cu^{2+}$ as templates and 3-aminopropyltriethoxysilane as a functional monomer, and the possible synergy mechanism was explored between dithizone coordination chemistry and multi-ion imprinting. The structures, morphologies and thermostability of MIIPs were well characterized by Fourier transform infrared (FT-IR), scanning electron microscopy (SEM), Brunauer–Emmett–Teller (BET) and thermogravimetry analysis (TGA). The resultant MIIPs showed high binding capacity and fast dynamics, and the adsorption processes obeyed Langmuir isotherm and pseudo-second-order dynamic models. The MIIPs displayed excellent selectivity toward the four target ions particularly over $Pb^{2+}$, $Zn^{2+}$ and $Co^{2+}$ with selective coefficients of 6.8–16.9, as well as high anti-interference ability when confronted with common co-present various ions. Moreover, a high preparation yield of 41% and good reusability over 90% desorption efficiency were obtained. Consequently, the MIIPs were used as solid-phase extraction sorbents for preconcentration of trace $Hg^{2+}$, $Cd^{2+}$, $Ni^{2+}$ and $Cu^{2+}$, presenting high detectability up to 6.0–22.5 ng $L^{-1}$ and satisfactory recoveries ranging from 94.7–110.2% in seawater samples. The developed MIIPs-based method proved to be a practically feasible method in heavy metal removal and water pretreatment.

Received 25th March 2016
Accepted 26th April 2016

DOI: 10.1039/c6ra07785d

www.rsc.org/advances



## 1. Introduction

Environmental pollutants like heavy metal ions have received widespread international concern, due to their bio-accumulation and non-biodegradability.[1] Heavy metal ions show a great trend to form complexes, especially with ligands of biological matter containing nitrogen, sulfur and oxygen, and thereby changing the molecular structures of proteins, breaking hydrogen bonds, or inhibiting enzymes.[1] Hence, there are ongoing efforts to develop various strategies for the analysis and removal of trace heavy metal ions, such as chemical precipitation,[2] adsorption,[3] ionic exchange,[4] electrochemical treatment,[5] and membrane separation techniques.[6] Nowadays, a novel effective strategy, ion imprinting technology (IIT), has been favored for recognition, determination and elimination of heavy metal ions at low concentrations in complicated matrices.[7–13]

IIT, an important branch of molecular imprinting technology, primarily targets ions as templates and combines the ligands or functional monomers to form chelates or composites based on electrostatic interaction and chelation, followed by the elution of template ions.[7,14,15] Then, the produced ion imprinted polymers (IIPs) possess the corresponding three-dimensional cavity structures complementary with the target ions.[7] IIPs are quite compatible with aqueous media which is remarkably advantageous over most MIPs, and can effectively identify, monitor, and remove targeted ions in aqueous/biological environments. Obviously in real cases, metal contamination is usually the combined pollution of several kinds of metal ions, for instance, the co-existent $Hg^{2+}$, $Cd^{2+}$, $Ni^{2+}$ and $Cu^{2+}$, with important environmental and toxicological significances, have become typical research targets. Multi-ion imprinting technology is able to treat the mixed pollutants in the same matrix simultaneously by retaining the recognition specificity for

[a]Key Laboratory of Life-Organic Analysis of Shandong Province, College of Chemistry and Chemical Engineering, Qufu Normal University, Qufu 273165, China

[b]Key Laboratory of Coastal Environmental Processes and Ecological Remediation, Yantai Institute of Coastal Zone Research, Chinese Academy of Sciences, Yantai 264003, China. E-mail: jhli@yic.ac.cn; lxchen@yic.ac.cn

[c]School of Pharmacy, Binzhou Medical University, Yantai 264003, China

† Electronic supplementary information (ESI) available. See DOI: 10.1039/c6ra07785d

specific target ion. The resultant multi-ion imprinted polymers (MIIPs) as potential materials to treat mixed pollutions, however, are still in infancy, and tough explorations are urgently required. To the best of our knowledge, there are very few MIIPs related researches and they are limited mostly to double-ion imprinting, such as Ce(IV)-Gd(III),[16] Cu(II)–Cd(II),[17] Cd(II)–Pb(II),[18] and As(V)–Cr(III)[19] dual-template IIPs. For example, Prasad *et al.* have fabricated double-ion imprinted polymer@magnetic nanoparticles modified screen printed carbon electrode for simultaneous analysis of Ce(IV) and Gd(III) ions.[16] The method is simple and cost-effective, and suitable for rapid detection.

Nevertheless, it's still difficult to obtain high selectivity for IIPs, because many metal ions have the similar ionic radius and properties and same charges, particularly to be embedded in flexible organic materials. Fortunately, silica, remarkably compatible with aqueous and biological systems, exhibits minimal swelling in the presence of solvents and shows excellent thermal stability, maintaining the shape and size of imprint cavities.[20] Sol–gel technology is an easy-to-handle and ecofriendly strategy, and can offer the possibility of tremendous control over the shape of the silica.[9,20] In addition, sol–gel process may make the contributions to high yield, because it is a more mature method without needless ingredients.

On the other hand, as a well-known traditional ligand, dithizone can form stable colored complexes with various metal ions including $Hg^{2+}$, $Cd^{2+}$, $Ni^{2+}$, $Cu^{2+}$, $Pb^{2+}$, $Zn^{2+}$, $Co^{2+}$, $Cr^{3+}$ and so on,[21–23] and has excellent selectivity advantages due to its –SH and –NH– functional groups.[9,12,21–25] The traditional view expects a tautomeric equilibrium for dissolved dithizone between the ketone form (Ph–NH–NH═CS–N═N–Ph) and the enol form (Ph–NH–N═C(SH)–N═N–Ph). As pH increases, it is easy for S with a lone-pair electron to bind with H to form a thiol group, which would easily form a complex with metal ions.[26] Put another way, the ketone form is dominant at lower pH while the enol form is dominant at higher pH. Furthermore, due to the presence of acidic thiol groups, the enol form is easy to release $H^+$ for coordination with metal ions at relatively higher pH.

By virtue of the synergy between dithizone coordination chemistry and multi-ion imprinting, we expect to propose a general IIPs strategy to analyze and remove diverse metal ions simultaneously. Novel MIIPs were synthesized by a facile sol–gel process using the mixture of $Hg^{2+}$, $Cd^{2+}$, $Ni^{2+}$ and $Cu^{2+}$ as a template, dithizone as a chelating agent, 3-aminopropyltriethoxysilane (APTES) as a functional monomer, and tetraethoxysilicane (TEOS) as a cross-linker. The structures, morphologies and thermostability of MIIPs were well characterized by Fourier transform infrared (FT-IR), scanning electron microscope (SEM), Brunauer–Emmett–Teller (BET) and thermogravimetry analysis (TGA). Static and dynamic adsorptions were systematically tested, and selectivity and anti-interference ability were investigated in detail. In addition, production yield and reusability of the material were assessed. Furthermore, the MIIPs were utilized as SPE sorbents and were successfully applied to the simultaneous extraction of $Hg^{2+}$, $Cd^{2+}$, $Ni^{2+}$ and $Cu^{2+}$ in seawater samples, providing a practically feasibly way for high throughput sample pretreatment and removal of trace heavy metal ions in complicated water matrices.

## 2. Experimental

### 2.1. Reagents and materials

Dithizone(diphenylthiocarbazone), TEOS and APTES were obtained from Sigma-Aldrich (Shanghai, China). Other reagents and materials were supplied by Sinopharm Chemical Reagent (Shanghai, China). All the reagents were at least analytical grade and were used directly without further purification, unless otherwise specified. Throughout the experiment aqueous solutions were prepared using doubly purified deionized (DDI) water, which was produced by a Milli-Q Ultrapure water system with the water outlet operating at 18.2 MΩ (Millipore, MA, USA); all pH measurements were performed using a pHs-3C digital pH meter equipped with a combined glass-calomel electrode (Shanghai, China).

### 2.2. Instrumentation

A FT-IR spectrometer (Thermo Nicolet Corporation, USA) was employed to record the infrared spectra of samples using a pressed KBr tablet method. UV-vis absorption spectra were measured on a Thermo Scientific NanoDrop 2000/2000C spectrophotometer (Thermo Fisher Scientific, Waltham, MA). A SEM (Hitachi S-4800, Japan, operating at 20 kV) was used to investigate the size and morphology of the MIIPs. The thermostability and purity was evaluated by TGA using a ZRY-2P thermal analyzer (Mettler Toledo). Specific surface area of the polymers was determined by BET analysis by performing nitrogen adsorption experiments, and the measurement was operated on an 3H-2000Ps2 (Beishide Instrument Technology (Beijing) Co., Ltd.). The polymers were degassed in vacuum at 150 °C prior to adsorption measurements. Atomic fluorescence measurements (AFS) of mercury were carried out with an AFS930 automatic sequential injection of atomic fluorescence spectrometer (Beijing Titan Instruments Co., China). Inductively Coupled Plasma Mass Spectrometry (ICP-MS) analyses were performed on a PerkinElmer Elan DRC II (USA).

### 2.3. Preparation of MIIPs

MIIPs were prepared by a sol–gel process. Briefly, hydrochloric acid was added into 150 mL ethanol and a pH = 6 solution was obtained. Dithizone (256 mg, 1 mmol) and the mixture of $Hg^{2+}$, $Cd^{2+}$, $Ni^{2+}$ and $Cu^{2+}$ individual at 0.1 mmol were dissolved in the above solution to form the chelates with continuous stirring for 1 h. Followed by adding APTES (700 μL) as functional monomers and stirring, preorganization proceeded at 4 °C in dark for 4 h. Then, TEOS (1.5 mL), as crosslinking agent, and aqueous ammonia (5 mL, 14%) were added in the mixing solution. The polymerization reaction was undertaken with magnetic stirring at room temperature for 12 h, and the product was further aged by stirring at 60 °C for 6 h to obtain high cross-linking density. The resultant MIIPs were filtered first and then washed with anhydrous ethanol for three times to remove the residues. 0.5 mol $L^{-1}$ HCl was used to treat the product under vigorous

 

stirring in order to remove the template ions. At last, the polymers were washed with DDI water to neutral and dried in vacuum to constant weight. The basic imprinting process was schematically illustrated in Fig. 1. For comparison, the non-imprinted polymers (NIPs) were also synthesized at the same manner, only in the absence of the template ions.

### 2.4. Adsorption experiments

Adsorption of 4 ions ($Hg^{2+}$, $Cd^{2+}$, $Ni^{2+}$, $Cu^{2+}$) from aqueous solutions was carried out in batch experiments. The static adsorption test was performed by allowing a constant amount of MIIPs to reach the adsorption equilibrium with $Hg^{2+}$, $Cd^{2+}$, $Ni^{2+}$ and $Cu^{2+}$ standard solution of known concentrations. That is, 20 mg MIIPs were dispersed in 10 mL standard solutions containing different amounts of target ions and incubated for 6 h under optimal sorption conditions. The mixture solutions were centrifuged at 7000 rpm. The supernatant solutions were collected and determined using AFS for $Hg^{2+}$ and ICP-MS for $Cd^{2+}$, $Ni^{2+}$ and $Cu^{2+}$, and the binding capacity ($Q$) of template ions was figured up by subtracting the free concentrations from the initial concentrations. AFS for mercury determination was regarded as more accurately. And similar experiments were carried out to investigate the effect of pH on adsorption capacity, in the multi-ion solutions with pH values ranging from 2 to 9 (adjusted using 0.1 mol $L^{-1}$ of phosphate buffer) at room temperature for 12 h. The pH was maintained in a range of $\pm$0.1 units.

In a meanwhile, the dynamic adsorption test was carried out by monitoring the temporal binding amount of ions as follows: 40 mg of IIPs was dispersed in 20 mL of 80 mg $L^{-1}$ ions standard solutions, and then the mixture was continuously oscillated for 0 to 150 min at room temperature in a thermostatically controlled oscillator. And then the further treatment was similar to that of the static adsorption test.

Selectivity experiments were conducted using $Pb^{2+}$, $Zn^{2+}$ and $Co^{2+}$ as comparison ions individually at the same concentration of 60 mg $L^{-1}$ as target ions, and interference tests were carried out using $K^{+}$, $Na^{+}$, $Ca^{2+}$, $Mg^{2+}$, $Zn^{2+}$, $Co^{2+}$ and $Pb^{2+}$ as concomitant ions individually at the concentration of 10 times excess (80 mg $L^{-1}$). The experimental processes were similar to the above static adsorption test.

### 2.5. MIIPs-SPE procedure

The prepared MIIPs (200 mg) were slurred with DDI water and then poured into a PTFE column for a SPE procedure. The column was preconditioned successively with 0.5 mol $L^{-1}$ HCl (5 mL), DDI water (10 mL) and 5 mL of blank solutions. Then the sample solutions (50 mL) containing target ions at three concentration levels (5, 10, and 15 μg $L^{-1}$) were respectively passed through the column at a flow rate of 1.0 mL $min^{-1}$. After that, the column was washed with DDI water (10 mL) and the adsorbate was eluted with 0.5 mol $L^{-1}$ HCl (2.5 mL). Finally, the obtained extractants were detected by AFS and ICP-MS.

### 2.6. Sample collection and preparation

Surface seawater samples were collected in a Teflon bottle from the Fisherman's Wharf of the Yellow Sea located in the coastal zone area of Yantai City. Samples were filtered through 0.45 μm PTFE syringe filters (Phenomenex, Los Angeles, CA, USA) to remove suspended particles. The resultant filtrates, which were directly analyzed or alkalified to pH 7.0 using 0.1 mol $L^{-1}$ NaOH, were kept in a refrigerator at 4 °C prior to use. Recoveries were investigated by spiking the $Hg^{2+}$, $Cd^{2+}$, $Ni^{2+}$ and $Cu^{2+}$ standards into seawater samples at three concentrations (5, 10 and 15 μg $L^{-1}$), and each concentration was analyzed five replicates, respectively.

## 3. Results and discussion

### 3.1. MIIPs preparation and proposed mechanism

The MIIPs were prepared by a sol–gel process, as illustrated in Fig. 1. As seen, the template ions, $Hg^{2+}$, $Cd^{2+}$, $Ni^{2+}$ and $Cu^{2+}$, encountered dithizone and formed chelates, and then, the functional monomer APTES was added. Here, the electron-donating amino N in APTES attacked the electron-deficient alkyl carbon on dithizone directionally, completing pre-

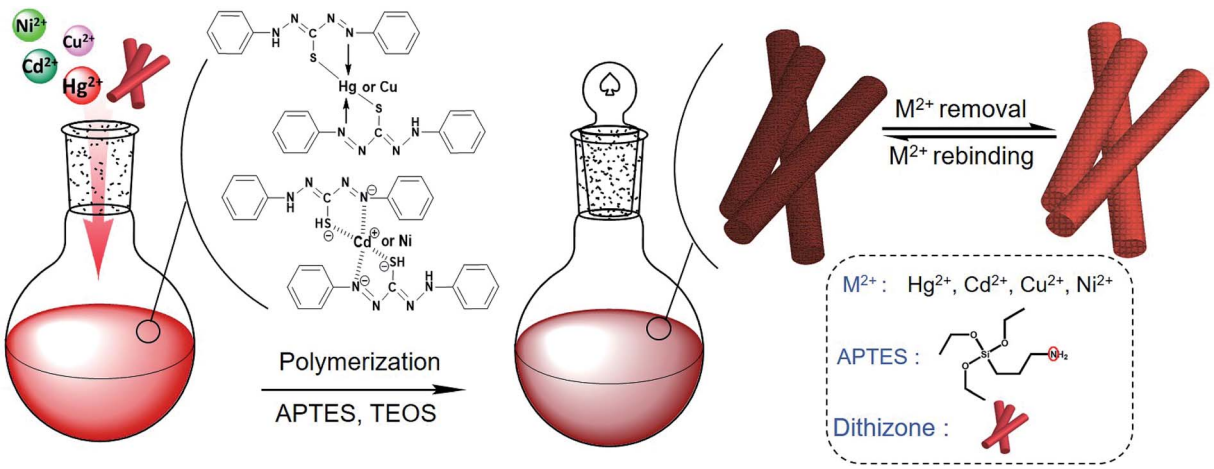


Fig. 1 Schematic illustration for preparation and imprinting process of MIIPs.

polymerization. An alkylating agent of TEOS was hydrolyzed by ammonia with the formation of four bare alcoholic hydroxyls. Alcoholic hydroxyl was employed to bond the electron-donating amino N in APTES, continuously polymerizing. Thus, APTES played a role of bridge or seed in the preparation of MIIPs. Finally, the template ions were removed by elution, leaving behind specific recognition sites in the polymers, with functional groups in a predetermined orientation and proper size cavities, which would contribute to the high adsorption efficiency and selectivity.[27]

The UV absorption spectra (Fig. 2A) and color changes (Fig. 2, insert) could reveal that strong chelation took place between dithizone and metal ions. Adding the same amount of ions to dithizone solution, the formed chelates presented distinct peak shift after combining with $Hg^{2+}$ or $Cu^{2+}$, as shown in Fig. 2A, suggesting a stronger covalent bond was generated between dithizone and $Hg^{2+}$; the chelates exhibited slight shift after coordination with $Cd^{2+}$ or $Ni^{2+}$ (Fig. 2A), suggesting the electrostatic interaction dominated between dithizone and ions. As displayed in Fig. 2B, the main ultraviolet absorption bands of dithizone in ethanol were 450 and 600 nm, while a large absorption peak appeared at about 480 nm and the absorption peak at 600 nm disappeared when metal ions were added, which proved the formation of metal chelates. Besides, after adding the moderate functional monomer APTES into chelates, the UV curve changed as well. All these observations suggested that dithizone could chelate the four metal ions and APTES could connect ligand dithizone and alkylating reagent TEOS.

### 3.2. Characterization of the MIIPs

Fig. S1† shows the FT-IR spectra of ions contained MIIPs, MIIPs and NIPs. The strong absorption band at around 1080 $cm^{-1}$ could be attributed to Si–O–Si antisymmetric stretching vibrations, and the absorption peaks at around 800 and 467 $cm^{-1}$ belonged to Si–O symmetrical stretching vibration and flexural vibration. These characteristic peaks in the three infrared spectra were all obvious, which indicated the presence of silica matrices in the three materials. The strong and broad absorption band observed at 3410 $cm^{-1}$ could be assigned to the N–H stretching vibration of APTES. Compared with NIPs, the characteristic absorption peak at 1625 $cm^{-1}$, which most probably represented the stretching vibrations of N=N double bonds in dithizone, became significantly weak in the MIIPs and ions contained MIIPs because they were coated. A new peak appeared at 1608 $cm^{-1}$ in ions contained MIIPs, which was just the characteristic peak of ion–N bond. All the results of FT-IR confirmed the presence of dithizone in the silica gel sorbents and its chelation with metal ions for imprinting.

Fig. 3 shows the SEM images of the MIIPs (A, B, C) and NIPs (D). As shown in Fig. 3B, the MIIPs displayed a dendritic structure and appeared to be covered with particles in several areas. Metal ions and dithizone formed the basic skeleton, firstly. Then further polymerization occurred in skeleton surface. However, in the absence of imprinting process, silicon particles easily aggregated (Fig. 3D). Hence, the dendritic-

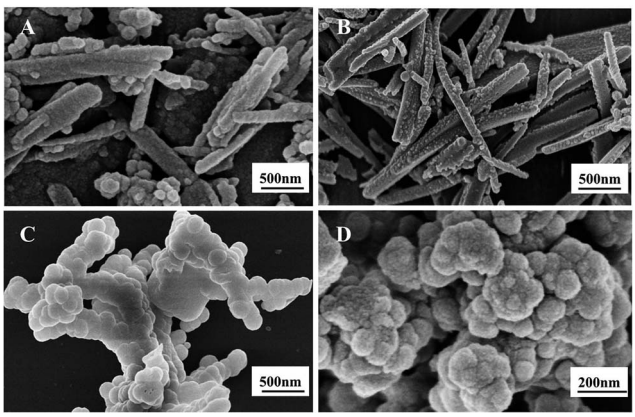


Fig. 3 Effect of different amounts of TEOS on the morphology of the polymer: (A) MIIPs using 1 mL TEOS, (B) MIIPs using 1.5 mL TEOS, (C) MIIPs using 2 mL TEOS, and (D) NIIPs using 1.5 mL TEOS.

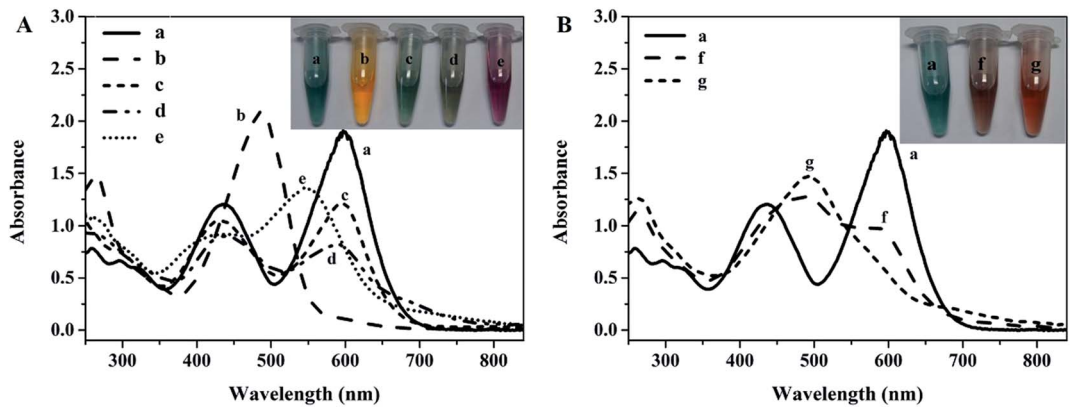


Fig. 2 (A) UV-vis spectra of dithizone alone (curve a, 0.1 mM), and $Hg^{2+}$ (curve b, 0.05 mM), $Cd^{2+}$ (curve c, 0.05 mM), $Ni^{2+}$ (curve d, 0.05 mM) and $Cu^{2+}$ (curve e, 0.05 mM) added into the dithizone solution, respectively. And the inset shows their corresponding solution photographs. (B) UV-vis spectra of dithizone alone (curve a, 0.1 mM), the dithizone (0.1 mM) with 4 ions (curve f, $Hg^{2+}$, $Cd^{2+}$, $Ni^{2+}$ and $Cu^{2+}$, 0.05 mM respectively), and APTES (6 μL) added into the dithizone (0.1 mM) with 4 ions (curve g, $Hg^{2+}$, $Cd^{2+}$, $Ni^{2+}$ and $Cu^{2+}$, 0.05 mM respectively). And the inset shows their corresponding solution photographs.

 

structured MIIPs were reasonable with partial coverage of silicon particles. Noticeably, the amount of TEOS as cross-linking agent would affect the number and distribution of bonding sites in the prepared polymer. Three typical dosages (1, 1.5 and 2 mL TEOS) were selected to optimize the experiments. As observed in Fig. 3A, individual silicon particles (secondary particles) existed in MIIPs using fewer amounts of TEOS. Fig. 3C shows the MIIPs for large amounts of TEOS; silicon particles were larger and agglomerate due to the excessive hydrolysis of TEOS. Fig. 3B shows the MIIPs, prepared by moderate amounts of TEOS, with plentiful cavity, bulge and rough surface, which is beneficial to adsorb target ions.

Fig. S2† shows the $N_2$ adsorption–desorption isotherms and pore size distribution of MIIPs and NIPs. By BET analysis, the specific surface area of MIIPs was attained as 15.59 $m^2\ g^{-1}$, much higher than that of the corresponding NIPs (4.62 $m^2\ g^{-1}$), as displayed in Table S1.† It should be noted, the specific surface area of MIIPs is lower than common MIPs especially spherical MIPs, which is very likely owing to the larger particle size of the polymer. The large size material does not occupy the advantage of large specific surface area compared with the micro-beads or nano materials, but two kinds of materials have their own advantages. Herein, the MIIPs material prepared in mild condition is simple in synthesis and can simultaneously specifically adsorb large amounts of metal ions, and more importantly, the MIIPs can be produced with high yield and thereby are feasible to large-scale practical applications, which are generally difficult to achieve by using micro-/nano-sized materials. On the other hand, the specific surface area of MIIPs was about three times as much as that in NIPs because of the lacuna or micro-aperture. So, imprinting cavities were proved to exist in the MIIPs. As seen from Fig. S2A,† when the relative pressure $P/P_0$ was less than 0.9, the slope of the curves was small, indicating that little amounts of small pores were present on the surface of MIIPs. However, when the relative pressure $P/P_0$ was higher than 0.9, the slope of the curves significantly increased and adsorption capacities increased obviously. As shown in Fig. S2B,† the average pore size for MIIPs and NIPs was 21.94 and 9.98 nm, respectively. Related morphological structure parameters of MIIPs and NIPs were listed in Table S1.† The large cumulative pore area was very likely because of the microspores on the surface of MIIPs, which revealed that the target ions were almost completely removed.

Fig. S3† shows the TG/DTG curves of MIIPs. With the increase of temperature from 50 to 100 °C, their weight loss was mainly owing to the evaporation and disappearance of adsorbed water. As the temperature changed from 100 to 200 °C, the weight decreased at a low loss rate, while ranging from 200 to 250 °C a high loss rate was displayed. The weight loss might well result from the decomposition and degradation of polymers. Consequently, the MIIPs were fully indicated to possess good thermal stability when the temperature was lower than 200 °C.

### 3.3. Binding studies of the MIIPs

Theoretically, the binding properties of MIIPs towards its template are dependent on the interaction between the ion and the ligand. Moreover, the chelation of dithizone is pH sensitive. So, the effects of pH on MIIPs performances were firstly investigated prior to static and dynamic binding studies. As shown in Fig. 4, within the scope of pH 2–9, adsorption capacity was determined with the pH change of the solutions. The adsorption capacity was low at pH below 4.0. The ketone form of dithizone was dominant and the N atoms were highly protonated at low pH, and hence, electronic-supply ability of N atoms was significantly weakened, reducing the chelating effect of dithizone for ions and leading to the low adsorption capacity.[17] With the increase of pH in 4–6, adsorption capacities of the two polymers were rapidly increased. The reason was very likely owing to that the ketone type coordination (Fig. 4I) gradually transformed into the enol type coordination (Fig. 4II). In other words, coordination mode was changed from 4-N to more stable 2-N & 2-S, which enhanced the adsorption capacity. When the pH was above 6.0, due to part of the ions forming metal hydroxide, adsorption capacity slowly descended. At pH > 9, the precipitation of metal ions occurred thoroughly because of hydrolysis. Therefore, to achieve high efficiency and good selectivity, a pH of 6 was chosen for material preparation. On the other hand, considering their possible applications in water treatment, pH 7.0 was selected for binding studies.

Furthermore, the choice was explained as follows. In the synthesis process, the partial acidic environment could avoid hydrolysis and precipitation to occur for the four ions, and then they could fully chelate with sufficient ligands in an enough reaction time span, ensuring the chelating to achieve balance. After sol–gel process, silica structures could provide a rigid protection for template ion and dithizone could provide chemical activity. Accordingly, effective imprinting could be guaranteed. In applications mostly to water treatment, the majority was for neutral and alkaline environments, so the chosen pH was appropriate. Finally, the optimal pH could be easily obtained simultaneously meeting the four kinds of ions, which took into accounts both the ligand dithizone ensuring full chelation, and the different ions satisfying their respective adsorption.

The static adsorption experiments were performed to evaluate the adsorption capacities of MIIPs and NIPs at the ions'

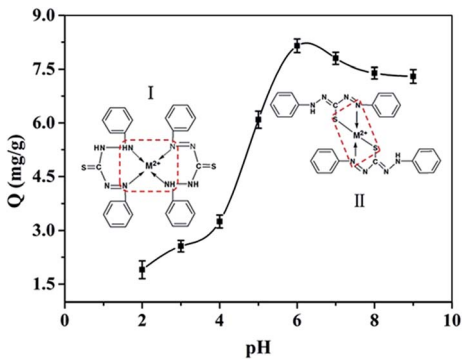


Fig. 4 Effect of pH on adsorption of target template ions for MIIPs. (Inset) (I) The chelate of dithizone ketone form with metal ions, (II) the chelate of dithizone enol form with metal ions ($M^{2+}$: $Hg^{2+}$, $Cd^{2+}$, $Ni^{2+}$, $Cu^{2+}$).

concentrations within 0–180 mg $L^{-1}$ from aqueous solutions with pH 7.0. As can be seen from Fig. S4A,† the amounts of ions adsorbed per unit mass of MIIPs increased with the increase of initial concentrations of template ions, and then hardly changed after 80 mg $L^{-1}$, indicating that the recognition sites were almost completely occupied by ions when exceeding the equilibrium concentration. The $Q_{max}$ (maximum adsorption capacity) from experiment was 16.55 mg $g^{-1}$. The adsorption capacities of MIIPs were much higher than that of NIPs, presenting a high imprinting factor ($\alpha$) of 5.34. This is because a large number of tailor-made imprinting cavities could specifically recognize template ions, while no matched cavities existed in NIPs only with low nonspecific adsorption.

The adsorption process was further studied by two classical isotherm models, Langmuir and Freundlich. Their corresponding equations and parameters for adsorption onto the MIIPs and NIPs were listed in Table S2.† The Langmuir model was found more suitable to the adsorption (Fig. S4B†), indicating that the target ions were adsorbed as a monolayer onto the surface of MIIPs.

Dynamic binding experiments were carried out to determine the binding rate and ion transfer properties. Fig. S4C† shows that the adsorption amounts of ions increased very fast in the initial 60 min and then slowed down gradually to an equilibrium state. Meanwhile, four models of the pseudo-first-order, pseudo-second-order, Elovich and intraparticle diffusion models were employed for fitting analysis, as shown in Fig. S4D.† It was seen that the pseudo-second-order model could better describe the time effect on the adsorption system, *i.e.*, predict the kinetic process, than other kinetic models, which provided the highest correlation coefficient of 0.996 as listed in Table S3.† The obtained equilibrium amounts (17.27 mmol $g^{-1}$) calculated from the model was in good agreement with that from experimental results (16.55 mmol $g^{-1}$). It could be expected that the rate-limiting step might be chemisorption involving valency forces through the sharing or exchange of electrons between sorbent and sorbate,[27] further confirming that the MIIPs were prepared based on metal–ligand coordination chemistry.[28]

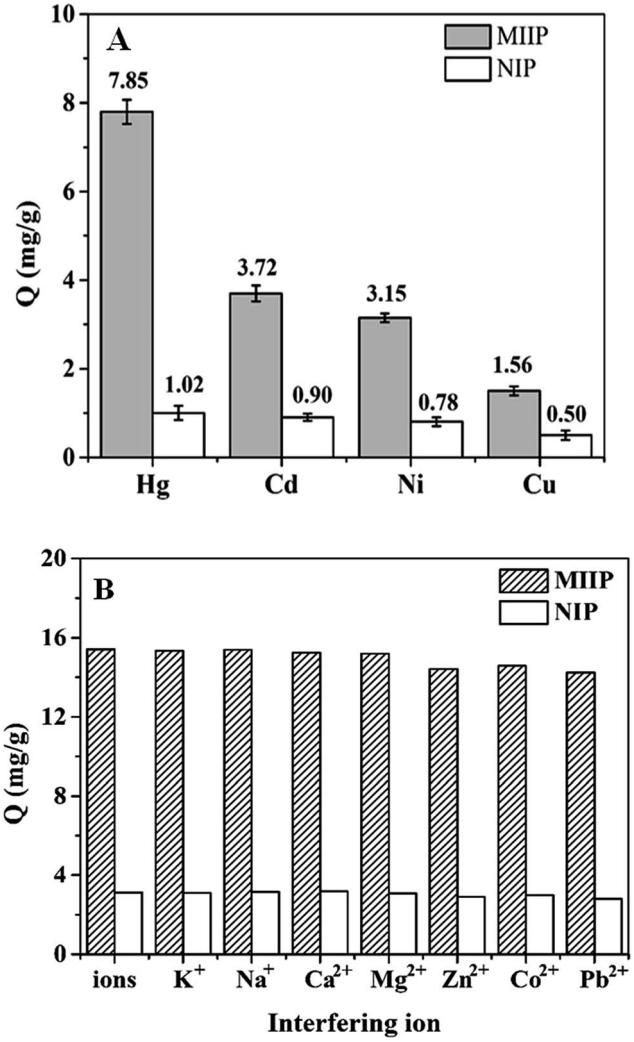


Fig. 5 (A) Adsorption capacity of MIIPs and NIPs for the target template $Hg^{2+}$, $Cd^{2+}$, $Ni^{2+}$, and $Cu^{2+}$. (B) Adsorption capacities for target template ions in the presence of interferential ions, including $K^+$, $Na^+$, $Ca^{2+}$, $Mg^{2+}$, $Zn^{2+}$, $Co^{2+}$ and $Pb^{2+}$, respectively. Experimental conditions: MIIPs or NIPs, 20 mg; V, 10 mL; sample solution, pH 7.0; metal ion concentration, 80 mg $L^{-1}$ respectively.

### 3.4. Selectivity and anti-interference examinations

In order to investigate the selectivity of MIIPs, the binding capacities of MIIPs to templates and other competitive ions were estimated. Fig. 5A shows the adsorption capacities of the MIIPs and NIPs for the four template ions. As observed, adsorption capacity of MIIPs for each ion was greater than that of NIPs, and the adsorption capacity order of MIIPs were $Q_{Hg} > Q_{Cd} > Q_{Ni} > Q_{Cu}$. Both metal–ligand chemistry and imprinting cavity were quite possibly responsible for the order. (1) There were different interaction between ligand and different ions owing to metal–ligand chemistry. When they reacted jointly, the reaction system needed to reach a balance, and the balance may bring about different amounts of effective cavities for the four different ions. Then, the amount of cavity would determine the adsorption capacity for each kind of ion. Under the condition of same ligand and environment, ion itself was responsible for the difference. Electrons released energy in the transfer process from the ligand to the metal cation, which made their combination more stable than the metal ion alone. Therefore, the electron accepting ability order ($Hg^{2+} > Ni^{2+} > Cd^{2+} > Cu^{2+}$) might account for the stability ordering of the chelated complexes. In reality, electron accepting ability has little difference, and it cannot completely determine the final adsorption order. On the other hand, the theory of soft and hard acids and bases (SHAB) may result in the order. It is well known that dithizone belongs to soft base and $Hg^{2+}$ or $Cd^{2+}$ belongs to soft acid. Their chelates are more stable than that of $Ni^{2+}$ or $Cu^{2+}$ which belongs to border acid. In the competitive adsorption of the four complexes, the complexes of $Hg^{2+}$ and $Cd^{2+}$ had slight superiority, and thereby leading to higher adsorption capacities. (2) Cavity was also an important factor for effective imprinting, and larger radius ion was more likely to be captured. Interestingly, the adsorption capacity followed the

 

same order as ionic radius. As a matter of fact, the different adsorption capacities for different ions by the MIIPs resulted from the co-influences of the abovementioned factors.

Competitive ion-recognition experiments were conducted by using $Pb^{2+}$, $Zn^{2+}$ and $Co^{2+}$ as competitive ions. These ions were chosen as they have the same charge, and strong bonding ability with dithizone, and they can coexist in aquatic environments, so they may be most likely to affect the imprinting process. As seen from Table 1, the competitive adsorption capacity of MIIPs for target ions was considerably higher than that of NIPs, which also proved the success of this imprinting method; the selectivity factors were achieved between 6.8 and 16.9. Therefore, the prepared MIIPs had an excellent selectivity for the four template ions.

For further study of the selectivity and reliability of the MIIPs, the adsorption capacities of template ions in the presence of 10 times concentrations of other possible interference ions, including $K^+$, $Na^+$, $Ca^{2+}$, $Mg^{2+}$, $Zn^{2+}$, $Co^{2+}$, and $Pb^{2+}$, respectively, were evaluated. Fig. 5B could suggest the binding sites of MIIPs for target ions only changed by 10%, which were occupied by the interfering ions. So, the possibly co-existent ions had no significant influence on the adsorption ability of MIIPs, and the MIIPs owned excellent selectivity and reliability.

### 3.5. Yield and reusability of the MIIPs

Besides the above-mentioned high selectivity and reliability, yield and reusability are also very important indexes, since they play key roles in improving the economic efficiency and thereby extending the practical applications of the MIIPs. In the present work, the yield ($Y$) of 41.35% calculated according to the following formula:

$$Y = m_p/\sum m_i \times 100\%, (i = 1, 2, 3,\ldots n) \quad (1)$$

where, $m_p$ and $m_i$ are the product mass after reaction and the mass of each component prior to polymerization, respectively, and $n$ is the number of components.

In fact, the present yield is quite high albeit seeming less dominant, even compared with that of a typical bulk polymerization which tends to gain a higher yield of 50% usually. As is well known, the monolithic polymers obtained by bulk polymerization has to be crushed, ground and sieved to an appropriate size, which leads to low affinity sites and destroys some high affinity binding sites, and confines their use as chromatographic adsorbents.[14,15] By contrast, sol–gel method enjoys several advantages: high purity and homogeneity, mild reaction condition and easy operation, manageable morphology and porosity, and strong abrasion resistance and physical rigidity.[20] As a more mature method without needless ingredient, sol–gel process in general is more competitive compared with other polymerization approaches. Therefore, the MIIPs could be produced by sol–gel polymerization with high yields.

Then, the reusability of MIIPs was also evaluated as shown in Fig. 6. Through 3 h treatment by using 0.5 mol $L^{-1}$ HCl as desorption medium, after repeating the adsorption–desorption cycle for 6 times, the desorption efficiencies over 90% of the adsorbed four ions from the MIIPs were obtained. On the other hand, the MIIPs displayed slight variances in adsorption capacities less than 4.6%. The results indicated the prepared novel MIIPs were excellently suited for reuse without remarkable decrease in their adsorption capacities for $Hg^{2+}$, $Cd^{2+}$, $Ni^{2+}$ and $Cu^{2+}$.

### 3.6. Analytical performance and applications of the MIIPs-SPE to water samples

The high yield and reusable MIIPs were employed as SPE sorbents. Under the optimized SPE conditions such as 1.0 mL $min^{-1}$ sample rate, 50 mL loading volume, and 5 mL of 0.5 mol $L^{-1}$ HCl for elution, the analytical performances based on MIIPs-SPE were investigated. Excellent linearity over the range of 0.1–15.0 μg $L^{-1}$ was attained, with the correlation coefficients above 0.9990 for the four ions. According to the IUPAC definition, the corresponding detection limits ($3\sigma$) of the method, defined as three times the standard deviation of the blank signal intensity, were 10.7, 6.0, 22.5 and 10.1 ng $L^{-1}$ for $Hg^{2+}$, $Cd^{2+}$, $Ni^{2+}$ and $Cu^{2+}$, respectively. Therefore, the developed MIIPs-SPE based method could realize highly sensitive detection of multiple analytes simultaneously.

Table 1 Selectivity of the prepared MIIPs and NIPs

| | MIIPs | | NIPs | |
|---|---|---|---|---|
| Ion | $D^a$ | $S^b$ | $D$ | $S$ |
| Template ions | 225.8 | — | 48.8 | — |
| $Pb^{2+}$ | 33.3 | 6.8 | 13.3 | 3.7 |
| $Zn^{2+}$ | 23.3 | 9.7 | 10.0 | 4.9 |
| $Co^{2+}$ | 13.3 | 16.9 | 9.2 | 5.3 |

[a] Distribution ratio, $D = Q/C_e$. [b] Selective coefficient, $S = D_{\text{template ion}}/D_{\text{competitive ion}}$. $D_{\text{template ion}}$ and $D_{\text{competitive ion}}$ are distribution ratio of the template and the competitive ions on MIIPs or NIPs, respectively.

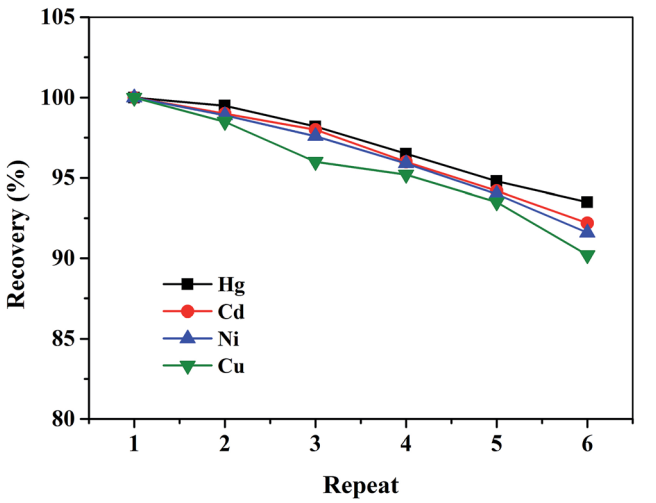


Fig. 6 Reusability of MIIPs for $Hg^{2+}$, $Cd^{2+}$, $Ni^{2+}$ and $Cu^{2+}$. Experimental conditions: MIIPs, 20 mg; V, 10 mL; sample solution, pH 7.0; metal ion concentration, 80 mg $L^{-1}$ respectively.

Table 2 MIIPs-SPE recoveries (%) and relative standard deviations (RSD, %) obtained from analysis of seawater samples spiked with $Hg^{2+}$, $Cd^{2+}$, $Ni^{2+}$ and $Cu^{2+}$[a]

| Ion | Adding ($\mu g\ L^{-1}$) | Found ($\mu g\ L^{-1}$) | Recovery[b] ± RSD[c] |
|---|---|---|---|
| Hg | 0 | 0.25 | — |
| | 5 | 5.51 | 110.20 ± 2.3 |
| | 10 | 10.03 | 100.30 ± 4.6 |
| | 15 | 14.92 | 99.47 ± 3.8 |
| Cd | 0 | 0.32 | — |
| | 5 | 5.29 | 105.80 ± 4.2 |
| | 10 | 9.66 | 96.60 ± 3.6 |
| | 15 | 14.20 | 94.67 ± 2.5 |
| Ni | 0 | 0.24 | — |
| | 5 | 4.84 | 96.80 ± 5.8 |
| | 10 | 10.22 | 102.20 ± 2.4 |
| | 15 | 15.80 | 105.33 ± 3.8 |
| Cu | 0 | 0.19 | — |
| | 5 | 4.95 | 99.00 ± 2.1 |
| | 10 | 10.23 | 102.30 ± 1.9 |
| | 15 | 14.42 | 96.13 ± 3.4 |

[a] Experimental conditions: loading volume, 50 mL; loading rate, 1 mL $min^{-1}$ washing, 10 mL of pure water; eluting, 5 mL of 0.5 mol $L^{-1}$ HCl. [b] Average value from five individual experiments. [c] $n = 5$.

Furthermore, the MIIPs were applied for the preconcentration and removal of trace $Hg^{2+}$, $Cd^{2+}$, $Ni^{2+}$ and $Cu^{2+}$ in seawater samples to evaluate the practicality of the developed method. The recovery was investigated by spiking with $Hg^{2+}$, $Cd^{2+}$, $Ni^{2+}$ and $Cu^{2+}$ standard at three levels (5, 10 and 15 $\mu g\ L^{-1}$) and analyzing five replicates for each concentration. As shown in Table 2, recoveries were in the range of 94.67–110.20%, with the relative standard deviation (RSD) of 1.9–5.8%, indicating the obtained MIIPs were greatly applicable for the effective preconcentration and removal of trace multiple ions in real water samples. The result also suggested that matrix effects could be remarkably reduced by virtue of the MIIPs-SPE procedure. Specifically, the endogenous contents of $Hg^{2+}$, $Cd^{2+}$, $Ni^{2+}$ and $Cu^{2+}$ were detected at 0.25, 0.32, 0.24 and 0.19 $\mu g\ L^{-1}$ in the tested seawater samples (Table 2). All the results validated the developed MIIPs-SPE method was potentially applicable for simultaneous separation and accurate quantitation of multiple trace heavy metal ions, and for high-effective monitoring and abatement of heavy metal pollution in complicated matrices.

## 4. Conclusions

In conclusion, the new four-ion templating MIIPs based on dithizone chelation were prepared by sol–gel polymerization, and were successfully applied to selectively pre-concentrate and remove trace $Hg^{2+}$, $Cd^{2+}$, $Ni^{2+}$ and $Cu^{2+}$ simultaneously in seawater samples. The developed four-ion templating strategy appears to be more advantageous over that reported dual-template imprinting methods as shown in Table S4,†[16–19] since more ions would lead to higher risks of cross-reactivity and matrix interferences. The most important feature of the present MIIPs is the multiple ions as a template using the same ligand and thereby providing novel multi-ion adsorption/separation substrates with high volume production, which will bring optimistic perspectives that various concerned species can be imprinted in a single polymer format for high throughput applications. The high throughput heavy metal ion analysis/removal IIPs-based platform can be constructed for the high effective monitoring and remediation of water quality.

## Acknowledgements

This work was financially supported by the Strategic Priority Research Program of the Chinese Academy of Sciences (XDA11020702), the National Natural Science Foundation of China (21275158, 21477160, 21575159) and the Project of on-site sediment microbial remediation of public area of central Bohai Sea, North China Sea Branch of State Oceanic Administration (QDZC20150420-002).

## Notes and references

1 G. Aragay, J. Pons and A. Merkoci, *Chem. Rev.*, 2011, **111**, 3433.
2 T. A. Kurniawan, G. Y. Chan, W. H. Lo and S. Babel, *Chem. Eng. J.*, 2006, **118**, 83.
3 J. H. Qu, *Chin. J. Environ. Sci.*, 2008, **20**, 1.
4 C. Jo, D. Pugal, I. K. Oh, K. J. Kim and K. Asaka, *Prog. Polym. Sci.*, 2013, **38**, 1037.
5 J. Grimm, D. Bessarabov and R. Sanderson, *Desalination*, 1998, **115**, 285.
6 G. M. Geise, H. S. Lee, D. J. Miller, B. D. Freeman, J. E. McGrath and D. R. Paul, *J. Polym. Sci., Part B: Polym. Phys.*, 2010, **48**, 1685.
7 J. Q. Fu, L. X. Chen, J. H. Li and Z. Zhang, *J. Mater. Chem. A*, 2015, **3**, 13598.
8 B. S. Zhao, M. He, B. B. Chen and B. Hu, *Spectrochim. Acta, Part B*, 2015, **107**, 115.
9 Z. Zhang, J. H. Li, X. L. Song, J. P. Ma and L. X. Chen, *RSC Adv.*, 2014, **4**, 46444.
10 C. C. Kang, W. M. Li, L. Tan, H. Li, C. H. Wei and Y. W. Tang, *J. Mater. Chem. A*, 2013, **1**, 7147.
11 S. F. Xu, L. X. Chen, J. H. Li, Y. F. Guan and H. Z. Lu, *J. Hazard. Mater.*, 2012, **237–238**, 347.
12 M. Saraji and H. Yousefi, *J. Hazard. Mater.*, 2009, **167**, 1152.
13 X. Q. Cai, J. H. Li, Z. Zhang, F. F. Yang, R. C. Dong and L. X. Chen, *ACS Appl. Mater. Interfaces*, 2014, **6**, 305.
14 L. X. Chen, S. F. Xu and J. H. Li, *Chem. Soc. Rev.*, 2011, **40**, 2922.
15 L. X. Chen, X. Y. Wang, W. H. Lu, X. Q. Wu and J. H. Li, *Chem. Soc. Rev.*, 2016, **45**, 2137.
16 B. B. Prasad and D. Jauhari, *Anal. Chim. Acta*, 2015, **875**, 83.
17 B. B. Prasad, D. Jauhari and A. Verma, *Talanta*, 2014, **120**, 398.
18 M. C. Barciela-Alonso, V. Plata-García, A. Rouco-López, A. Moreda-Piñeiro and P. Bermejo-Barrera, *Microchem. J.*, 2014, **114**, 106.
19 L. Y. Zhu, Z. L. Zhu, Y. L. Qiu and R. H. Zhang, *Sep. Sci. Technol.*, 2014, **49**, 1584.
20 J. E. Lofgreen and G. A. Ozin, *Chem. Soc. Rev.*, 2014, **43**, 911.

 

21 Y. M. Leng, Y. L. Li, A. Gong, Z. Y. Shen, L. X. Chen and A. G. Wu, *Langmuir*, 2013, **29**, 7591.
22 M. Jamshidi, M. Ghaedi, K. Dashtian and S. Hajati, *RSC Adv.*, 2015, **5**, 105789.
23 Y. Xi, Y. T. Luo, J. M. Luo and X. B. Luo, *J. Chem. Eng. Data*, 2015, **60**, 3253.
24 J. J. Deng, X. J. Kang, L. Q. Chen, Y. Wang, Z. Z. Gu and Z. H. Lu, *J. Hazard. Mater.*, 2011, **196**, 187.
25 M. E. Mahmoud, M. M. Osman, O. F. Hafez, A. H. Hegazi and E. Elmelegy, *Desalination*, 2010, **251**, 123.
26 Y. Wang, J. Xie, Y. C. Wu, H. L. Ge and X. Y. Hu, *J. Mater. Chem. A*, 2013, **1**, 8782.
27 Y. S. Ho and G. McKay, *Process Biochem.*, 1999, **34**, 451.
28 J. J. Becker and M. R. Gagne, *Acc. Chem. Res.*, 2004, **37**, 798.